shown as a pocket that encloses the porphyrin macrocycle on all sides except one. Since iron binding occurs via vicinal sulfhydryls prior to porphyrin binding, it should be possible for both substrates to freely associate. The observation that the size of substituents at the 2- and 4-positions is limiting supports a binding area enclosed or restricted at that end, and the lack of inhibition by N-substituted porphyrins with alkyl groups larger than two carbons suggests that a region surrounding the top and bottom of the porphyrin ring exists. The tryptophan residue(s) is (are) present in the pocket, exposed to surrounding water, but poorly accessible to the bulk solvent phase and is (are) in proximity to the MIANS. The presence of a porphyrin binding pocket rather than a more open, hydrophilic site is compatible with the physical properties of protoporphyrin, which is poorly soluble in aqueous solution and readily partitions into hydrophobic solvents. The properties described above for ferrochelatase are also similar to those detailed for heme binding pockets in hemoproteins. It is interesting to speculate about the similarities between ferrochelatase and hemoproteins since all bind tetrapyrroles and may share common structural features. Complete evaluation of this, however, must await further structural studies including the amino acid sequence of ferrochelatase.

References

Anderson, S. R., Brunori, M., & Weber, G. (1970) *Biochemistry 9*, 4723–4729.

Andley, U. P., Liang, J. N., & Chakrabarti, B. (1982) *Biochemistry 21*, 1853–1858.

Argos, P., & Rossman, M. G. (1979) *Biochemistry 18*, 4951–4960.

Dailey, H. A. (1982) *J. Biol. Chem. 257*, 14714–14718.

Dailey, H. A. (1984) *J. Biol. Chem. 259*, 2711–2715.

Dailey, H. A., Jr., & Lascelles, J. (1974) *Arch. Biochem. Biophys. 160*, 523–529.

Dailey, H. A., & Fleming, J. E. (1983) *J. Biol. Chem. 258*, 11453–11459.

Dailey, H. A., & Smith, A. (1984) *Biochem. J. 223*, 441–445.

DeMatteis, F., Gibbs, A. H., & Smith, A. G. (1980) *Biochem. J. 189*, 645–648.

Eftink, M. R., & Ghiron, C. A. (1976) *Biochemistry 15*, 672–680.

Eftink, M. R., & Ghiron, C. A. (1981) *Anal. Biochem. 209*, 199–227.

Gupte, S. S., & Lane, L. K. (1979) *J. Biol. Chem. 254*, 10362–10367.

Hanson, J. W., & Dailey, H. A. (1984) *Biochem. J. 222*, 695–700.

Harbin, B. M., & Dailey, H. A. (1985) *Biochemistry* (in press).

Honeybourne, C. L., Jackson, J. T., & Jones, O. T. G. (1979) *FEBS Lett. 98*, 207–210.

Hudson, E. H., & Weber, G. (1973) *Biochemistry 12*, 4154–4161.

Kunze, K. L., Mangold, B. L., Wheeler, C., Beilan, H. S., & Ortiz de Montellano, P. R. (1983) *J. Biol. Chem. 458*, 4202–4207.

Lakowicz, J. R. (1983) in *Principles of Fluorescence Spectroscopy* (Lakowicz, J. R., Ed.) Plenum Press, New York.

Penefsky, H. S. (1977) *J. Biol. Chem. 252*, 2891–2899.

Prendergast, F. G., Meyer, M., Carlson, G. L., Iida, S., & Potter, J. D. (1983) *J. Biol. Chem. 258*, 7541–7544.

Stern, O., & Volmer, M. (1919) *Phys. Z. 20*, 183.

Stryer, L. (1965) *J. Mol. Biol. 13*, 482–495.

Taketani, S., & Tokunaga, R. (1981) *J. Biol. Chem. 256*, 12748–12753.

Increased Stability of the Higher Order Structure of Chicken Erythrocyte Chromatin: Nanosecond Anisotropy Studies of Intercalated Ethidium

Ikuo Ashikawa, Kazuhiko Kinosita, Jr., and Akira Ikegami*

The Institute of Physical and Chemical Research, Hirosawa 2-1, Wako-shi, Saitama 351, Japan

Yoshifumi Nishimura and Masamichi Tsuboi

Faculty of Pharmaceutical Sciences, University of Tokyo, Hongo, Bunkyo-ku, Tokyo 113, Japan

Received May 29, 1984

ABSTRACT: Internal motion of the DNA in chicken erythrocyte chromatin fibers was studied by measurement of the fluorescence anisotropy decay of ethidium intercalated in the linker region. A comparison of the decay curves of the dye in chicken erythrocyte chromatin with those of calf thymus chromatin [Ashikawa, I., Kinosita, K., Jr., Ikegami, A., Nishimura, Y., Tsuboi, M., Watanabe, K., Iso, K., & Nakano, T. (1983) *Biochemistry 22*, 6018–6026] revealed greater suppression of nucleosome movement in chicken erythrocyte chromatin. Furthermore, the transition of this chromatin to the compact (solenoidal) structure occurred at lower solvent concentrations of Na^+ or Mg^{2+} than those for calf thymus chromatin. These results demonstrated increased stability of the higher order structure (the solenoid) of chicken erythrocyte chromatin, which may be related to the reduction of nuclear activity in the chicken erythrocyte cell. In addition to intact chicken erythrocyte chromatin, we studied the structural transitions of H1-depleted and H1,H5-depleted chromatins. The result indicated that histone H5 of this chromatin stabilizes the higher order structure in the presence of magnesium (or divalent) cation and did not induce the transition in the solution containing only sodium cation.

Internal motion of DNA in solution has been investigated recently by NMR (Early & Kearns, 1976; Hogan & Jardetzky, 1979, 1980; Bolton & James, 1980; Opella et al., 1981), fluorescence depolarization (Wahl et al., 1970; Thomas et al., 1980; Millar et al., 1980, 1982), ESR (Robinson et al., 1980), and triplet anisotropy decays (Hogan et al., 1982,

0006-2960/85/0424-1291$01.50/0

1983). From among these techniques, fluorescence depolarization studies of intercalated ethidium have revealed DNA motions in the nanosecond regime, of which the main component was considered to be torsional motion of the DNA rod (Barkley & Zimm, 1979; Allison & Schurr, 1979). Recently, this technique has been applied to studies of the internal motion of the DNA rod complexed with proteins, such as DNA in chromatin (Genest et al., 1982; Wang et al., 1982; Ashikawa et al., 1983a,b) and DNAs in bacteriophage heads (Ashikawa et al., 1984). In these studies, anisotropy decay measurement of intercalated ethidium was verified to be a sensitive tool for the investigation of the mode or strength of the DNA–protein or DNA–DNA interaction.

During erythropoiesis in nucleated erythrocytes, pronounced structural and functional changes occur in the chromatin. The appearance of the tissue-specific histone H5 (Weintraub, 1978) is accompanied by a reduction in nuclear activity. In the mature erythrocyte, transcription is barely detectable (Zentgraf et al., 1975) and H1 has been replaced by, or supplemented with, substantial amounts of H5, which has a higher arginine content than H1 (Briand et al., 1980). It might be expected that such a profound modification would be reflected in the physical properties of the chromatin compared with that from the more active nuclei of rat liver or calf thymus.

We have previously examined the DNA motion in calf thymus chromatin (Ashikawa et al., 1983b) and showed that the salt-induced structural transition of chromatin from the extended form to the solenoidal one was reflected in the anisotropy decays of ethidium intercalated in the linker DNA. Here, we investigate the rigidity of chromatin structure in its extended and condensed form, and we study the Na^+- or Mg^{2+}-induced structural transition of chicken erythrocyte chromatins (intact, H1 depleted, and H1,H5 depleted) by using depolarization measurements. Using our results, we discuss the stabilization of the higher order structure of chicken erythrocyte chromatin compared with that of chromatin from other tissue. We also discuss how H1 and H5 contribute to the stabilization of the higher order structure of chromatin fibers as well as their roles in the transition from the extended to the solenoidal forms.

Materials and Methods

Preparation of Chicken Erythrocyte Chromatins and DNA. Chicken erythrocyte nuclei and chromatin were prepared by the method of Olins et al. (1976) with the following modification: the isolated nuclei were washed with 10 mM tris(hydroxymethyl)aminomethane (Tris), 10 mM NaCl, 3 mM $MgCl_2$, and 1 mM phenylmethanesulfonyl fluoride (PMSF), pH 7.5, several times. For the preparation of long chromatin, the nuclei (A_{260} = 50 OD units) were digested with micrococcal nuclease (40 units/mL) at 37 °C. After the nuclease was removed from the nuclei, the nuclei were disrupted in 1 mM Tris/1 mM ethylenediaminetetraacetic acid (EDTA) at pH 7.5. The outpoured chromatin was washed with 0.15 M NaCl, 1 mM Tris, and 1 mM EDTA, pH 7.5 and then was applied to a Sepharose 6B column. Only fractions eluted near the void volume were taken as the desired sample. Removal of histone H1 was performed by ultracentrifugation of this chromatin in 0.55 M NaCl, 10 mM Tris, 0.2 mM EDTA, and 0.5 mM PMSF, pH 7.5 (35000 rpm, 16 h), over a cushion of several milliliters of 30% sucrose, 0.55 M NaCl 10 mM Tris, and 0.2 mM EDTA, pH 7.5. In this ultracentrifugation, the sample concentration was adjusted to be higher than 3.0 mg of DNA/mL, since under this concentration histone H5 began to separate from the long chromatin. After ultracentrifugation, the pelleted chromatin was dispersed in 5 mM Tris/0.2 mM EDTA, pH 7.5, dialyzed against this buffer, applied to the Sepharose 6B column. Removal of histone H1 and H5 was performed by two ultracentrifugations of the chromatin in 0.65 M NaCl, 10 mM Tris, and 0.2 mM EDTA, pH 7.5 (35000 rpm, 16 h). In this case also, the sample was loaded over the cusion of 30% sucrose, 0.65 N NaCl, 10 mM Tris, and 0.2 mM EDTA, pH 7.5. After each ultracentrifugation, the chromatin pellet was solubilized in 5 mM Tris/0.2 mM EDTA, pH 7.5, and was dialyzed against this buffer. We used chromatography to remove short chromatin; we applied H1,H5-depleted chromatin to the Sepharose 6B column and took the fractions eluted near the void volume. To prevent nucleosome rearrangements in H1-depleted and in H1,H5-depleted chromatin, we always treated the samples at 2–4 °C. In order to check whether or not the nucleosome rearrangement occurred in H1,H5-depleted chromatin, we digested our sample with micrococcal nuclease and observed the nuclease cutting pattern of the extracted DNA of the digested sample via polyacrylamide gel electrophoresis. The digestion of the sample produced the discrete DNA fragments characteristic of native chromatin, indicating that extensive nucleosome rearrangement does not occur in our sample.

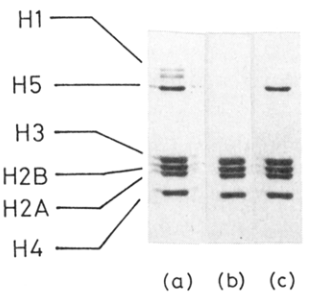

FIGURE 1: Sodium dodecyl sulfate/polyacrylamide gel electrophoresis patterns of the histone from the samples: (a) intact chromatin; (b) H1,H5-depleted chromatin; (c) H1-depleted chromatin.

In order to check the integrity of the histone proteins in these samples, electrophoresis in sodium dodecyl sulfate/polyacrylamide gel of the histones was carried out on 18% slab gels, as described by Laemmli (1970). Electrophoresis patterns are shown in Figure 1. Lengths of DNAs in these chromatin samples were determined by measuring sedimentation coefficients of the isolated DNAs. The obtained sedimentation coefficients were 14–20 S in 5 mM Tris, 100 mM NaCl, and 1 mM EDTA, pH 7.5 at 20 °C, and the molecular weights were thought to range between 3.3×10^6 and 6.5×10^6.

Long DNA was isolated from chicken erythrocyte nuclei by method of Kay et al. (1952). The sedimentation coefficient of this DNA was 19.8 S in 5 mM Tris, 100 mM NaCl, and 1 mM EDTA, pH 7.5 at 20 °C, and the molecular weight was thought to be about 6.5×10^6.

Measurement of Fluorescence. Measurements of the time courses of the fluorescence anisotropy and those of the steady-state fluorescence anisotropy were performed with a single photon counting apparatus. Details of the system and measurement conditions have already been described (Kinosita et al., 1981; Ashikawa et al., 1983b).

Buffer conditions of the chromatin samples were 1 mM Tris/0.2 M EDTA, pH 7.5, and the concentration of Na^+ or Mg^{2+} in the samples was adjusted by adding NaCl or $MgCl_2$ solutions of appropriate concentrations. Anisotropy decay of cell nuclei suspension was measured in 10 mM Tris, 10 mM NaCl, and 3 mM $MgCl_2$, pH 7.5. Concentrations of the samples were within 0.1~0.3 mg of DNA/mL. Ethidium bromide was added so that P/D ([phosphate]/[dye]) ranged between 1500 and 3000. At these low concentrations of the

added dye, energy transfer between the intercalated dyes was found to be negligible (Ashikawa et al., 1983b). In the case of cell nuclei suspension, measurements of several different concentrations of the samples were made in order to check whether the scattering from the sample influenced the anisotropy decay curve or not; the result showed that the scattering did not affect the decay curve in the concentration range of the sample mentioned above. In fluorescence measurements, the sample cuvette (1 cm × 1 cm) was always kept at 20 °C. We measured the anisotropy decay of the samples within a few days after the isolation.

Analysis of Fluorescence Data. Characterization of the internal motion of DNA free in solution and in chromatin was made following the analysis described earlier (Ashikawa et al., 1983b). The major part of the anisotropy decay of the intercalated ethidium has been considered to arise from the torsional motion of the DNA (Barkley & Zimm, 1979; Allison & Schurr, 1979). For DNA in solubilized chromatin and in cell nuclei, the observed anisotropy decay, $R(t)$, is represented as follows:

$$r(t) = r_i(t)r_w(t) = r_0\{a_1 \exp[-(t/\varphi_1)^{1/2}] + a_2\} \exp(-t/\varphi_2) \quad (1)$$

In this expression, parameters a_2 ($=1 - a_1$) and φ_1 are related to the length (L) between the fixed ends, the torsional rigidity (C) of the DNA rod, and the friction (ρ) per unit length of the DNA ($\rho = 4\pi b^2\eta$) (b is the radius of the DNA).

The least-squares analysis gave experimental parameters for the internal motion, a_2 and φ_1. These two parameters allow the estimation of L/C and $L\rho$. The values of L, C, and ρ (or the effective viscosity η) themselves, however, can be fixed unless further assumptions are made. This is an inherent property of our model; a $r_i(t)$ vs. t curve is given by only two parameters.

The affinity of the dye to DNA was reduced when the DNA was in a cell nucleus, and only 70% of the added dyes could be intercalated in the DNA. We therefore subtracted the fluorescence component of the free dye from the observed fluorescence decay curve prior to the least-squares analysis as described earlier (Ashikawa et al., 1984).

Results and Discussion

Dynamics of DNA in Chicken Erythrocyte Chromatin. The structure of chromatin has been reported to be sensitive according to the ionic constituents of the solvent and the presence of small amounts of Ca^{2+} or Mg^{2+} (Thoma et al., 1979; McGhee et al., 1980). At moderate ionic strength (50–200 mM NaCl) or in the presence of Ca^{2+} or Mg^{2+}, chromatin assumes a compact "solenoid structure" (Finch & Klug, 1976), while at very low ionic strength and in the absence of divalent cations it assumes an extended form. We showed, in the previous paper (Ashikawa et al., 1983b), that these structural transitions of chromatin were reflected in the anisotropy decays of intercalated ethidium. In this subsection, we describe the results of the anisotropy decay measurements of the dye in intact chicken erythrocyte chromatin. We compare the stability of the higher order structure of this chromatin with that of calf thymus chromatin.

Figure 2 shows the anisotropy decay curves of ethidium in chicken erythrocyte chromatin. These decay curves should reflect the motion of the linker DNA, because in chromatin the ethidium dye has been known to be intercalated exclusively in the linker DNA if the added dye concentration is relatively low (Paoletti et al., 1977; Erard et al., 1979; Genest et al., 1981a,b). With higher dye concentrations, we observed extensive energy transfer among the intercalated dyes. We

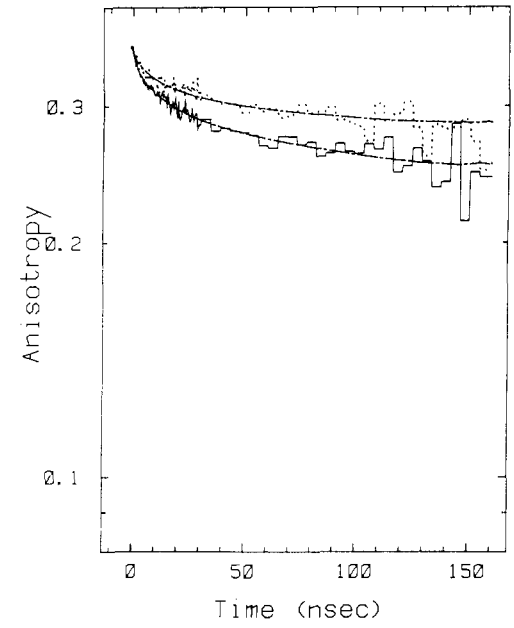

FIGURE 2: Fluorescence anisotropy decay curves of intercalated ethidium in intact chicken erythrocyte chromatin. Buffer conditions were 1 mM Tris 0.2 mM EDTA, pH 7.5 (solid line), and 50 mM NaCl, 1 mM Tris, and 0.2 mM EDTA, pH 7.5 (dotted line). The temperature in the cuvette was 20 °C. P/D = 1500–3000. The anisotropy values after 30 nm are averaged over 10 channels; 1 ns equals 2.32 channels. Chain lines are the least-squares fits with eq 1 to the observed decays.

concluded that the ethidium dye was actually intercalated in the narrow region in the chromatin DNA, probably the linker region. The anisotropy decay of chromatin in 50 mM NaCl was suppressed more than in 1 mM Tris. This suppression is thought to result from the restriction of the internal motion of the linker DNA and decreased nucleosome mobility in the condensed form of the chromatin. In the absence of 50 mM NaCl, the motion of the intercalated dye must occur easily, since the chromatin assumes the extended form in which the linker DNA is extended and there is no core–core interaction. In the presence of 50 mM NaCl the linker DNA is thought to be bent and core–core interaction emerges, both of which suppress the anisotropy decay of the intercalated dye. This observed difference in the decay profiles was the same as the difference observed in calf thymus chromatin. However, in chicken erythrocyte chromatin each of these anisotropy decays (in 1 mM Tris and in 50 mM NaCl) was suppressed more than that in calf thymus chromatin. These differences suggest that chicken erythrocyte chromatin is in a more rigid conformation than calf thymus chromatin.

By fitting eq 1 to the observed decay curves in Figure 2, we decomposed the decay curves into the one corresponding to the internal motion, $r_i(t)$, and that resulting from the movement of nucleosomes in chromatin, $r_w(t)$. This procedure allows independent quantitative estimation of the rigidity of the linker DNA and the stability of the chromatin higher order structure. Chain lines in Figure 2 are the resultant least-squares fitting curves to the observed decays. The calculated parameters [a_2 ($= 1 - a_1$), φ_1, and φ_2] are tabulated in Table I.

From the a_2 value, we could calculate the movable angle (the standard deviations of the torsional fluctuation) of the DNA only in the linker region (Ahikawa et al., 1983b). A seen in the $\Delta\gamma$ values of chicken erythrocyte chromatin and calf thymus chromatin (Table II), the internal motion of the linker DNA of chicken erythrocyte chromatin was only slightly more restricted than that in calf thymus chromatin; the dif-

Table I: Parameters [ϕ_1, ϕ_2, a_2 (=1 − a_1)] Calculated by Fitting Eq 1 to the Measured Anisotropy Decay Curves of the Samples

	ϕ_1 (ns)	ϕ_2 (ns)	a_2 (=1 − a_1)
CE[a] chromatin in 1 mM Tris	10.53	1100	0.775
CE chromatin in 50 mM NaCl	12.16	2500	0.824
CE chromatin in 0.47 mM $MgCl_2$	7.34	2500	0.842
CE H1-depleted chromatin in 1 mM Tris	7.38	705	0.748
CE H1-depleted chromatin in 50 mM NaCl	8.49	800	0.764
CE H1-depleted chromatin in 0.77 mM $MgCl_2$	9.56	2500	0.785
CE H1,H5-depleted chromatin in 1 mM Tris	8.01	550	0.708
CE H1,H5-depleted chromatin in 50 mM NaCl	9.83	600	0.660
CE H1,H5-depleted chromatin in 2 mM $MgCl_2$	9.60	600	0.731
CE nuclei	5.84	2500	0.804
CT chromatin in 1 mM Tris[b]	12.00	450	0.721
CT chromatin in 50 mM NaCl[b]	5.85	1100	0.815

[a] CE and CT represent chicken erythrocyte and calf thymus, respectively. [b] Ashikawa et al. (1983b).

ference in the mobility of the linker DNA in these two kinds of chromatin was thus relatively small. From φ_2, we can obtain information about stability of the higher order structure. If chromatin is in a rigid solenoidal form and core–core interaction is strong, the calculated φ_2 value will be larger than that for flexible chromatin fiber. As seen in Table I, the calculated φ_2 values of chicken erythrocyte chromatin in both its extended (in 1 mM Tris) and condensed (in 50 mM NaCl) forms were larger than those , respectively, of calf thymus chromatin (Ashikawa et al., 1983b). This shows that H1 and H5 in chicken erythrocyte chromatin suppress the motion of the chromatin fiber mainly by making a more stable higher order structure than H1 in calf thymus chromatin. In the presence of 0.47 mM $MgCl_2$, the anisotropy decay of chicken erythrocyte chromatin was more suppressed than that in 50 mM NaCl (Table I).

Dynamics of DNA in H1-Depleted and in H1,H5-Depleted Chromatin. It has been thought that histones H1 and H5 have roles for maintenance of the chromatin higher order structure. In the absence of these proteins, chromatin cannot assume the solenoidal structure (Thoma et al., 1979). Furthermore, these histones are thought to stabilize core DNA in chromatin (Fulmer & Fasman, 1979; Cowman & Fasman, 1980; Watanabe & Iso, 1980).

Among these two histones, we are interested in the role of H5 for maintenance of the solenoid structure, because this additional histone has been thought to be responsible for the transcriptional inactivity of the mature erythrocyte. Kumar & Walker (1980) investigated the dissociation of histone H1 and H5 from chicken erythrocyte chromatin at various salt concentrations. They concluded that H5 has a greater affinity for chromatin DNA than does H1. This may be due to the higher proportion of arginine residues in this histone, although tne total number of basic residues in H1 and H5 is roughly the same. Thomas & Rees (1983) reported preferential affinity of H5 for chromatin that assumes the higher order structure. Recently, Thoma et al. (1983) showed greater affinity of the globular domain of H5 than that of H1 to chromatin DNA and suggested that the globular domain of H1 served as a temporary seal and that of H5 as a permanent seal of the nucleosome. Besides these reports, however, there is little information about how this additional histone contributes to the maintenance of the chromatin higher order structure

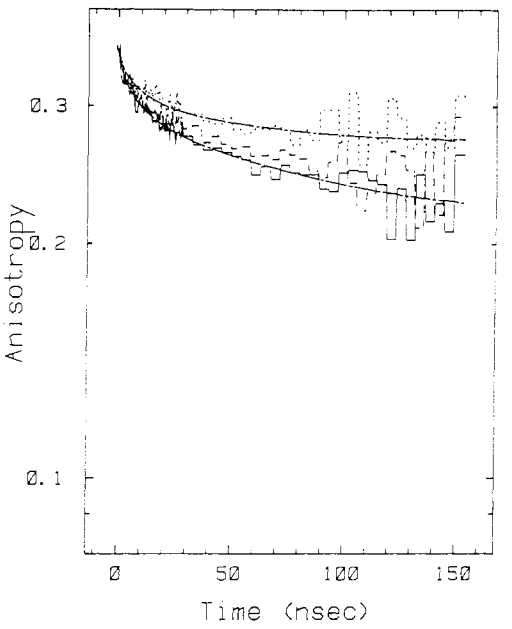

FIGURE 3: Fluorescence anisotropy decay curves of intercalated ethidium in H1-depleted chicken erythrocyte chromatin. Buffer conditions were 1 mM Tris 0.2 mM EDTA, pH 7.5 (solid line), 50 mM NaCl, 1 mM Tris, and 0.2 mM EDTA, pH 7.5 (dashed line), and 0.77 mM $MgCl_2$, 1 mM Tris, and 0.2 mM EDTA., pH 7.5 (dotted line), at 20 °C. P/D = 1500–3000. Chain lines are the least-squares fits with eq 1 to the observed decays of the samples in 1 mM Tris and in 0.77 mM $MgCl_2$.

In order to clarify the role of H1 and H5 in stabilization of the higher order structure of chromatin fiber, we examined the movement of the linker DNA of H1-depleted chromatin, in which histone H5 remained. Figure 3 shows the anisotropy decay curves of intercalated ethidium in H1-depleted chro-

Table II: Estimated Torsional Angles of Linker DNAs and Obtained Relationships among the Length (L), the Torsional Rigidity (C), and the Effective Viscosity (η) of Movable DNAs in Chicken Erythrocyte Chromatins

	movable angle, $\Delta\gamma$ (deg)	L/C (erg^{-1})	$L\eta$ (cm·P)
CE[a] chromatin in 1 mM Tris	14.5	8.8×10^{12} (1.3×10^{13})[b]	1.1×10^{-7} (1.0×10^{-7})
CE chromatin in 50 mM NaCl	10.8	6.6×10^{12} (9.9×10^{12})	1.7×10^{-7} (1.5×10^{-7})
CE chromatin in 0.47 mM $MgCl_2$	9.6	5.9×10^{12} (8.8×10^{12})	1.1×10^{12} (1.0×10^{-7})
CE H1-depleted chromatin in 1 mM Tris	16.6	1.0×10^{13} (1.5×10^{13})	6.8×10^{-8} (6.4×10^{-8})
CE H1-depleted chromatin in 50 mM NaCl	15.3	9.4×10^{12} (1.4×10^{13})	9.2×10^{-8} (7.9×10^{-8})
CE H1-depleted chromatin in 0.77 mM $MgCl_2$	13.7	8.4×10^{12} (1.2×10^{13})	1.0×10^{-7} (9.8×10^{-8})
CE H1,H5-depleted chromatin in 1 mM Tris	20.0	1.2×10^{13} (1.8×10^{13})	6.2×10^{-8} (6.0×10^{-8})
CE H1,H5-depleted chromatin in 50 mM NaCl	24.5	1.5×10^{13} (2.2×10^{13})	6.4×10^{-8} (6.4×10^{-8})
CE H1,H5-depleted chromatin in 2 mM $MgCl_2$	18.0	1.1×10^{13} (1.6×10^{13})	8.2×10^{-8} (7.8×10^{-8})
CE nuclei	12.2	7.5×10^{12} (1.1×10^{13})	7.1×10^{-8} (6.6×10^{-8})
CT chromatin in 1 mM Tris[c]	16.9	1.0×10^{13} (1.5×10^{13})	9.5×10^{-8} (1.0×10^{-7})
CT chromatin in 50 mM NaCl[c]	11.6	7.1×10^{12} (1.1×10^{13})	7.5×10^{-8} (7.1×10^{-8})

[a] CE and CT represent chicken erythrocyte and calf thymus, respectively. [b] Values in parentheses were calculated with the assumption of random distribution of the dye in the linker DNAs. [c] Ashikawa et al. (1983b).

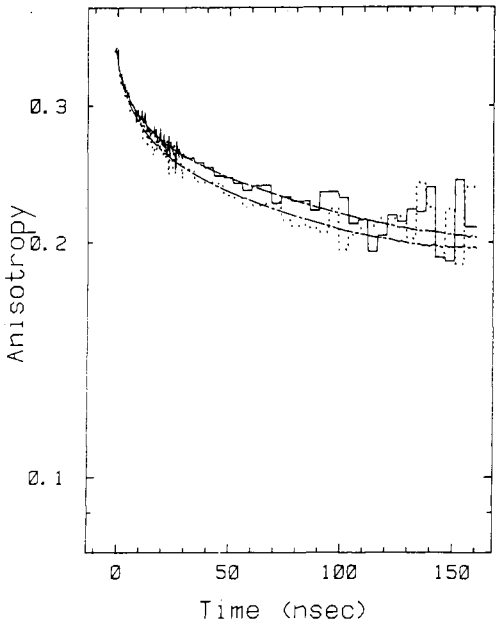

FIGURE 4: Fluorescence anisotropy decay curves of intercalated ethidium in H1,H5-depleted chicken erythrocyte chromatin. Buffer conditions were 1 mM Tris/0.2 mM EDTA, pH 7.5 (solid line), and 50 mM NaCl, 1 mM Tris, and 0.2 mM EDTA, pH 7.5 (dotted line), at 20 °C. P/D = 1500–3000. Chain lines are the least-squares fits with eq 1 to the observed decays of the samples in 1 mM Tris and in 50 mM NaCl.

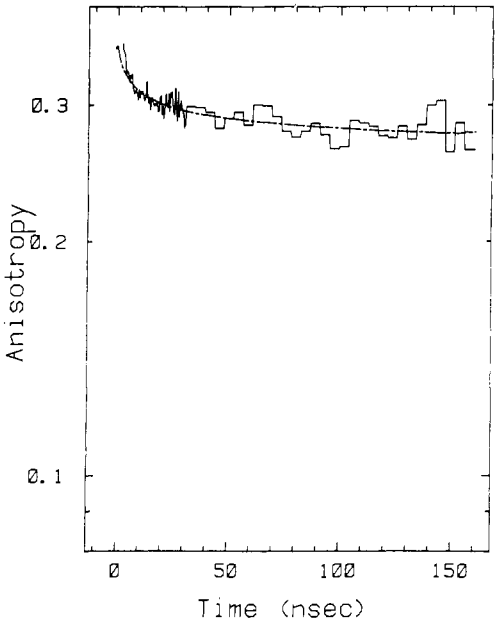

FIGURE 5: Fluorescence anisotropy decay curve of intercalated ethidium in chicken erythrocyte nuclei. Buffer condition was 10 mM Tris, 10 mM NaCl, and 3 mM $MgCl_2$, pH 7.5. at 20 °C. P/D = 2000. Sample concentration was 0.3 mg of DNA/mL. Chain line is the least-squares fit with eq 1 to the observed decay.

matin. In 1 mM Tris, the anisotropy decayed more extensively than that of intact chromatin (Figure 2). This enhanced decay can be attributed to the absence of H1 in this chromatin. From the results of the least-squares fittings, we see that both the nucleosome movements and the internal motions of the linker region were enhanced.

The most important conclusion obtained from the anisotropy measurements of H1-depleted chromatin was that this sample was induced into the solenoidal form only by Mg^{2+} but not by Na^+. The anisotropy decay curve of H1-depleted chromatin in 50 mM NaCl was only slightly suppressed as compared with that in 1 mM Tris, while the decay in 0.77 mM Mg^{2+} was largely suppressed. The φ_2 value in Table I shows that in 0.77 mM Mg^{2+} nucleosome movement was suppressed to almost the same extent as that of intact chromatin. Therefore, it was concluded that histone H5 and histone H1 play a different role in maintenance of the condensed form of chromatin; histone H5 stabilized the solenoidal form only in the presence of Mg^{2+}. Since we could not obtain a chromatin sample in which only histone H1 remained, we cannot discriminate, at present, whether occurrence of the salt-induced transition to the compact form requires only histone H1 or both H1 and H5.

Figure 4 shows the anisotropy decay curves of ethidium in H1,H5-depleted chromatin. From these decay curves, we recognize that even in the presence of 50 mM NaCl or several hundred micromolar Mg^{2+} there is no suppression of the anisotropy decay of the sample as compared with that in 1 mM Tris (Table I).

Dynamics of DNA in Chromatin in Nuclei. In cell nuclei, the dye is probably exclusively intercalated in chromatin DNA and not in RNA, because the measured lifetime of ethidium in cell nuclei (≈22.6 ns) is much closer to its lifetime in DNA than in RNA (≈27 ns). Furthermore, the lifetime of the dye in disrupted nuclei in 1 mM Tris (≈23.8 ns) was found to be identical with that in isolated chromatin in the same buffer. As it was found that an intercalating probe was bound in the linker region in chromatin in cell nuclei (Cech & Karrer, 1980), the ethidium dye is also thought to be intercalated in the linker region in cell nuclei.

Figure 5 shows the anisotropy decay curve of ethidium in the linker region of chromatin in chicken erythrocyte cell nuclei. Here, the anisotropy decay is found to be largely suppressed, almost to the same extent as in solubilized intact chromatin in its solenoidal form. This result demonstrates that in cell nuclei the first higher order structure of chromatin is similar to that found in intact chromatin of its solenoidal form. In other words, the solubilization of chromatin from cell nuclei with nuclease digestion does not seem to change the factors that maintain the compact structure of chromatin in cell nuclei.

Analysis of the Internal Motion of the Linker Region, $r_i(t)$. We discuss, in the subsection, the torsional motion of the linker DNA in three different preparations of chromatins (intact, H1 depleted, and H1,H5 depleted) in a somewhat more quantitative manner. The procedure of the analysis was described under Materials and Methods.

We do not know the actual binding site of ethidium in the linker DNA in chromatin. Let us first assume that the dye molecule is *bound in the midpoint* of the DNA in the linker region (Ashikawa et al., 1983b).

The calculated values of L/C and $L\eta$ (on this assumption) are tabulated in Table II. If one wants to estimate each of these values (L, C, and η) independently, one must estimate one of these three values by taking the structure of chromatin and the flexibility of the DNA into account.

If we assumed that the torsional rigidities of the linker DNAs of the extended forms of the three preparations of chromatins (intact, H1 depleted, and H1,H5 depleted) in 1 mM Tris are equal to that of free DNA in the same buffer (1.8×10^{-19} erg·cm),[1] we can calculate the movable length of the DNA and the effective viscosiy around it. The calculated lengths of the movable DNA are 45 base pairs (bp) for the case of intact chromatin, 53 bp for H1-depleted chromatin,

[1] This value was calculated with the assumption that the hydrodynamic radius of the DNA rod was 1.35 nm and that the angle of the transition moments of the dye to the axis of the DNA (ϵ) was 90°. If we assumed ϵ = 70°, the torsional rigidity would be reduced by about 10%.

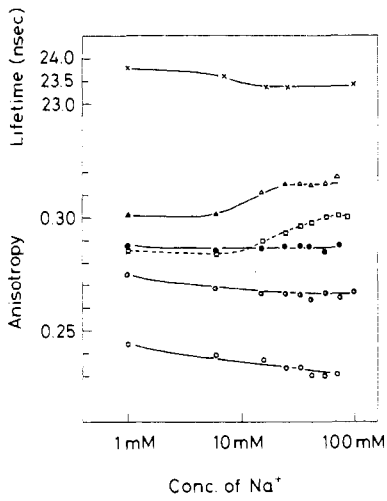

FIGURE 6: Steady-state fluorescence anisotropy values of intercalated ethidium in intact chicken erythrocyte chromatin (triangles), in H1-depleted chromatin (closed circles), in H1,H5-depleted chromatin (half-closed circles), and in chicken erythrocyte DNA (open circles) at various concentrations of NaCl. Squares are the steady-state anisotropy values of ethidium in intact calf thymus chromatin, which are redrawn from our previous work (Ashikawa et al., 1983b). Buffer conditions were 1 mM Tris/0.2 mM EDTA, pH 7.5, and the concentrations of the samples were 0.1–0.2 mg of DNA/mL. P/D = 2000–3000; the temperature was held at 20 °C.

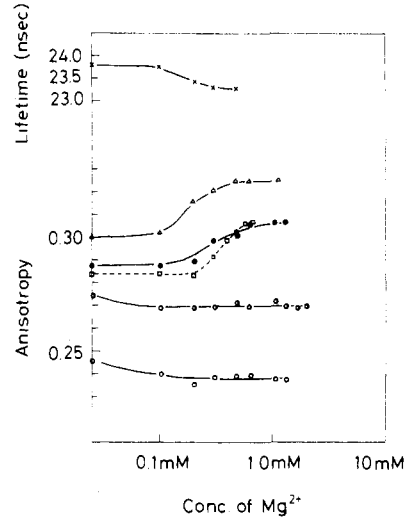

FIGURE 7: Steady-state fluorescence anisotropy values of intercalated ethidium in intact chicken erythrocyte chromatin (triangles), H1-depleted chromatin (closed circles), H1,H5-depleted chromatin (half-closed circles), and isolated chicken DNA (open circles) at various molar concentrations of $MgCl_2$. Squares are the steady-state anisotropy values of the dye in intact calf thymus chromatin, which are redrawn from our previous work (Ashikawa et al., 1983b). Buffer conditions, the sample concentrations, and P/D values were the same as those of Figure 6.

and 65 bp for H1,H5-depleted chromatin. An increase in the movable length by about 10 bp has been observed in each step on going from the intact chromatin to H1,H5-depleted chromatin. The calculated effective viscosity around the linker DNAs were 0.066 P for intact chromatin, 0.039 P for H1-depleted chromatin, and 0.028 P for H1,H5-depleted chromatin. Here, a decrease in the effective viscosity has been found on the sequential dissociation of histone H1 and H5.

Let us now examine the consequences of assuming *uniform distribution of the dye* in the linker DNA. The resulting calculated L/C and $L\eta$ are shown in parentheses in Table II. The L/C values for the uniform binding are about 1.5 times as large as that of the midpoint binding, and the $L\eta$ values for the uniform binding are reduced by factor of about 0.9.

Transition of Chromatins from Extended to Condensed Forms. As mentioned in the previous subsections, the overall structural change of chromatin is reflected in the extent of the mobility of the linker DNA. Using this probe, we examined how the structural transitions of three different preparations of chicken erythrocyte chromatins (intact, H1 depleted, H1,H5 depleted) take place with increasing ionic strength in the solvents. Bates et al. (1981) investigated the sedimentation velocity changes of chicken erythrocyte chromatin caused by the increase in ionic strength of the solvent. They compared the transition of the chromatin conformation of chicken erythrocyte chromatin with that of rat liver chromatin (Butler & Thomas, 1980) and concluded that they are similar as far as the changes in the sedimentation coefficients are concerned.

In Figure 6, triangles represent the steady-state anisotropy values of ethidium intercalated in the linker DNA in intact chromatin at various NaCl concentrations. Similarly, closed circles are the anisotropy values of H1-depleted chromatin, half-closed circles are those of H1,H5-depleted chromatin, and open circles are those of isolated DNA from chicken erythrocyte. For comparison, the anisotropy values of calf thymus chromatin obtained in our previous work (Ashikawa et al., 1983b) are also plotted (square). Motions of the linker DNA of intact chromatin are increasingly suppressed as the concentration of Na^+ increases. This transition reflects the structural change of chromatin to the condensed form. The midpoint of the transition is at 12.6 mM NaCl, while for calf thymus chromatin, the midpoint of the transition is at 23.6 mM. The transition of chicken erythrocyte chromatin occurs at much lower ionic strength than that of calf thymus chromatin: the condensed form of the former was stabilized more readily by Na^+ than that of the latter. This difference in the stabilization of the condensed form must be caused by a stronger condensation ability of chicken erythrocyte H1 (since histone H5 alone cannot induce the transition by Na^+) or of a cooperation of histone H1 and H5.

Figure 7 shows the steady-state anisotropy values of intact chicken erythrocyte chromatin (triangle), H1-depleted chromatin (closed circles), H1,H5-depleted chromatin (half-closed circles), isolated chicken erythrocyte DNA (open circles), and calf thymus chromatin (squares) (Ashikawa et al., 1983b) at various $MgCl_2$ concentrations. With Mg_2^+ also, the transition of intact chicken erythrocyte chromatin to the solenoidal form occurs at lower concentration of Mg^{2+} than that of calf thymus chromatin.

For H1-depleted chromatin, the effects of Na^+ and Mg^{2+} are different (see closed circles in Figure 7). With Mg^{2+}, an anisotropy increase in H1-depleted chromatin takes place at nearly the same concentration as that of anisotropy increase of the intact chromatin, while with Na^+ such an increase does not take place (see closed circles in Figure 6).

For H1,H5-depleted chromatin as well as for free chicken DNA, the anisotropy values decrease as the concentration of Na^+ or Mg^{2+} increased. This should be caused by the decrease in the rigidity of DNA in higher ionic strength solvents.

As was shown in our previous paper (Ashikawa et al., 1983b), the fluorescence lifetime of the intercalated ethidium depends upon the conformational state of DNA. The transition of chromatin observed by the steady-state anisotropy change was reflected also in lifetime changes of intercalated ethidium (Figures 6 and 7), and the midpoints of the lifetime changes coincided with those of the anisotropy changes.

CONCLUSIONS

We showed, in this paper, a higher stability of the condensed form of chicken erythrocyte chromatin than the corresponding

form of calf thymus chromatin. This increased stability of the higher order structure of the chromatin may be one of the molecular mechanisms of gene inactivation in chicken erythrocyte nuclei. We propose that anisotropy measurement of intercalated dyes can be applied to investigate the change in the stability of the chromatin higher order structure accompanying cell proliferation, aging, and cell transformation.

ACKNOWLEDGMENTS

We thank Dr. H. Akutsu, S. Nishimoto, and M. Shirakawa of Osaka University for their aid in performing gel electrophoresis of the chromatin DNA. We also thank Dr. J. Marque of The Institute of Physical and Chemical Research for critical reading of the manuscript.

Registry No. Mg, 7439-95-4.

REFERENCES

Allison, S. A., & Schurr, J. M. (1979) *Chem. Phys. 41*, 35–59.
Ashikawa, I., Kinosita, K., Jr., Ikegami, A., Nishimura, Y., Tsuboi, M., Watanabe, K., & Iso, K. (1983a) *J. Biochem. (Tokyo) 93*, 665–668.
Ashikawa, I., Kinosita, K., Jr., Ikegami, A., Nishimura, Y., Tsuboi, M., Watanabe, K., Iso, K., & Nakano, T. (1983b) *Biochemistry 22*, 6018–6026.
Ashikawa, I., Furuno, T., Kinosita, K., Jr., Ikegami, A., Takahashi, H., & Akutsu, H. (1984) *J. Biol. Chem. 259*, 8338–8345.
Barkley, M. D., & Zimm. B. H. (1979) *J. Chem. Phys. 70*, 2991–3007.
Bates, D. L., Butler, P. J. G., Pearson, E. C., & Thomas, J. O. (1981) *Eur. J. Biochem. 119*, 469–476.
Bolton, P. H., & James, T. L. (1980) *J. Am. Chem. Soc. 102*, 25–31.
Briand, G., Kmiecik, D., Sautiere, P., Wouters, D., Borie-Loy, O., Biserte, G., Mazen, A., & Champagne, M. (1980) *FEBS Lett. 112*, 147–151.
Butler, P. J. G., & Thomas, J. O. (1980) *J. Mol. Biol. 140*, 505–529.
Cech, T. R., & Karrer, K. M. (1980) *J. Mol. Biol. 136*, 395–416.
Cowman, M. K., & Fasman, G. D. (1980) *Biochemistry 19*, 532–541.
Earley, T. A., & Kearns, D. R. (1979) *Proc. Natl. Acad. Sci. U.S.A. 76*, 4170–4174.
Erard, M., Das, G. C., de Murcia, G.., Mazen, A., Pouyet, J., Champagne, M., & Daune, M. (1979) *Nucleic Acids Res. 6*, 3231–3252.
Finch, J. T., & Klug, A. (1976) *Proc. Natl. Acad. Sci. U.S.A. 73*, 1897–1901.
Fulmer, A. W., & Fasman, G. D. (1979) *Biopolymers 18*, 2875–2891.
Genest, D., Sabeur, G., Wahl, Ph., & Auchet, J.-C. (1981a) *Biophys. Chem. 13*, 77–87.
Genest, D., Sabeur, G., Wahl, Ph., & Aubel-Sadron, G. (1981b) *Biophys. Chem. 13*, 89–96.
Genest, D., Wahl, Ph., Erard, M., Champagne, M., & Daune, M. (1982) *Biochemie 64*, 419–427.
Hogan, M. E., & Jardetzky, O. (1979) *Proc. Natl. Acad. Sci. U.S.A. 79*, 6341–6345.
Hogan, M. E., & Jardetzky, O. (1980) *Biochemistry 19*, 2079–2085.
Hogan, M., Wang, J., Austin, R. H., Monitto, C. L., & Hershkowitz, S. (1982) *Proc. Natl. Acad. Sci. U.S.A. 79*, 3518–3522.
Hogan, M., LeGrange, J., & Austin, B. (1983) *Nature (London) 304*, 752–754.
Kay, E. R. M., Simmons, N. S., & Dounce, A. L. (1952) *J. Am. Chem. Soc. 74*, 1724–1726.
Kinosita, K. J., Kataoka, R., Kimura, M., Gotoh, O., & Ikegami, A. (1981) *Biochemistry 20*, 4270–4277.
Kumar, N. M., & Walker, I. O. (1980) *Nucleic Acids Res. 8*, 3535–3551.
Laemmli, U. K. (1970) *Nature (London) 227*, 680–685.
McGhee, J. D., Rau, D. C., Charney, E., & Felsenfeld, G. (1980) *Cell (Cambridge, Mass.) 22*, 87–96.
Millar, D. P., Robbins, R. J., & Zewail, A. H. (1980) *Proc. Natl. Acad. Sci. U.S.A. 77*, 5593–5597.
Millar, D. P., Robbins, R. J., & Zewail, A. H. (1982) *J. Chem. Phys. 76*, 2080–2094.
Olins, A. L., Carlson, R. D., Wright, E. B., & Olins, D. E. (1976) *Nucleic Acids Res. 3*, 3271–3291.
Opella, S. J., Wise, W. B., & DiVerdi, J. A. (1981) *Biochemistry 20*, 284–290.
Paoletti, J., Magee, B. B., & Magee, P. T. (1977) *Biochemistry 16*, 351–357.
Robinson, B. H., Lerman, L. S., Beth, A. H., Fisch, H. L., Dalton, L. R., & Auer, C. (1980) *J. Mol. Biol. 139*, 19–44.
Thoma, F., Koller, Th., & Klug, A. (1979) *J. Cell Biol. 83*, 403–427.
Thoma, F., Losa, R., & Koller, Th. (1983) *J. Mol. Biol. 167*, 619–640.
Thomas, J. C., Allison, S. A., Appellof, C. J., & Schurr, J. M. (1980) *Biophys. Chem. 12*, 177–188.
Thomas, J. O., & Rees, C. (1983) *Eur. J. Biochem. 134*, 109–115.
Wahl, Ph., Paoletti, J., & Lepecq, J.-B. (1970) *Proc. Natl. Acad. Sci. U.S.A. 65*, 417–421.
Wang, J., Hogan, M., & Austin, R. H. (1982) *Proc. Natl. Acad. Sci. U.S.A. 79*, 5896–5900.
Watanabe, K., & Iso, K. (1981) *J. Mol. Biol. 151*, 143–163.
Weintraub, H. (1978) *Nucleic Acids Res. 5*, 1179–1188.
Zentgraf, H., Scheer, U., & Franke, W. W. (1975) *Exp. Cell Res. 96*, 81–95.